

**NASA
Technical
Paper
2788**

1988

Performance of a Small,
Graphite Electrode,
Multistage Depressed
Collector With a 500-W,
Continuous Wave, 4.8- to
9.6-GHz Traveling Wave Tube

Peter Ramins,
Gary G. Lesny,
Ben T. Ebihara,
and Shelly Peet

*Lewis Research Center
Cleveland, Ohio*



National Aeronautics
and Space Administration

Scientific and Technical
Information Division

Summary

A small, isotropic graphite multistage depressed collector (MDC) and a short permanent magnet refocuser were designed, fabricated, and evaluated in conjunction with a 500-W, continuous-wave (CW), 4.8- to 9.6-GHz traveling-wave tube (TWT). A novel performance optimization system and technique were used to optimize the TWT-MDC performance for saturated broad-band operation. The MDC performance was evaluated in both four- and three-stage configurations. Average TWT overall and four-stage collector efficiencies of 43.8 and 82.6 percent, respectively, were obtained for saturated octave-bandwidth operation. The isotropic graphite electrode material performed well, and shows considerable promise. However, considerably more test experience is required before definitive conclusions on its suitability for space or airborne TWT's can be made.

Introduction

In the TWT-MDC performance optimization studies reported in reference 1, very high efficiencies were obtained with a small-sized, computer designed MDC operated in conjunction with a medium power, broad-band TWT. In this laboratory demonstration there were four elements which were not considered practical for production model TWT's as follows:

- (1) A relatively long variable spent beam refocuser, consisting of two coils.
- (2) A carbon black coating on the MDC electrode surfaces to minimize secondary electron emission losses.
- (3) An overly large passive support structure for the water-cooled MDC electrodes.
- (4) An extra (nonfunctional) length to the TWT-MDC introduced by the use of the ultra-high-vacuum (UHV) valve between the refocuser output and the MDC.

These deficiencies were addressed in a subsequent technology demonstration program. The computer-aided design techniques described in reference 2 were used to design a small-sized MDC and a short permanent magnet refocuser for the same model TWT. Techniques were devised to produce a complete (packaged) isotropic graphite MDC assembly (ref. 3), sufficiently small to fit within the outline (envelope) of the existing production model TWT-MDC and conductively cooled to the same baseplate. The permanent magnet refocuser and graphite electrode MDC were built and evaluated in

conjunction with a version of the same basic TWT for which they were designed. A comparison of the computed and measured TWT-MDC performance is presented in reference 4. This paper presents the following:

- (1) A brief description of the design and fabrication concepts and techniques for the graphite electrode MDC assembly.
- (2) A novel TWT-MDC performance optimization system and technique suitable for use in a TWT production line.
- (3) The TWT-MDC performance over its operating band of 4.8 to 9.6 GHz and its dynamic range.

Symbols

f	operating frequency, GHz
I_{en}	current to n th collector electrode, mA
I_G	total current to TWT body (ground), mA
I_0	cathode or beam current, mA
P_b	sum of beam interception losses and circuit losses, W
P_{RF}	total RF output power, W
P_{rec}	recovered power in collector, W
V_{en}	voltage on n th collector electrode, with respect to ground, V
V_0	cathode voltage with respect to ground, V
η_{ov}	overall TWT efficiency, $\sum_{n=1}^4 \frac{P_{RF}}{(V_0 - V_{en})I_{en} + I_G V_0}$, percent
η_{RF}	RF efficiency, $P_{RF}/V_0 I_0$, percent

Design, Fabrication, and Performance Evaluation Program

Overall Program

The program included the design, fabrication, and performance evaluation of a small four-stage, graphite electrode collector, and a spent beam refocuser in conjunction with a CW TWT (Teledyne MEC model MTH-5065). The MDC was designed and assembled at NASA Lewis Research Center. The components of the collector assembly were fabricated by T MEC (Teledyne MEC). The design effort included both the active section (electrode geometry) and the passive electrode support structure (including cooling, high

voltage (HV) stand-off, and vacuum envelope designs) of an isotropic graphite electrode MDC.

The MDC was joined to the TWT body, baked out, focused, and brought up to CW operation at T MEC. The bakeout performance, the early RF-dc beam processing (outgassing) performance, and initial TWT-MDC performance were noted in a log supplied by T MEC. Final focusing of the TWT (according to a new procedure discussed in a subsequent section of this report), and the optimization and evaluation of the TWT-MDC performance were performed at NASA Lewis.

TWT Characteristics

The general characteristics of T MEC model MTH-5065 are shown in table I for the low (CW) mode. The TWT is nominally a dual-mode tube with a relatively small (2 dB) pulse-up capability in RF output power. However, the TWT and MDC were optimized for the low mode and, except for the results reported in reference 4, testing was limited to the low (CW) mode.

MDC and Refocuser Characteristics

The geometry of the active portion of the MDC and typical operating potentials are shown in figure 1. The electrodes were made of high-purity isotropic graphite; the electrode surfaces were not modified further after the machining operation. The MDC was designed to fit within the envelope of the existing production model TWT, and be conductively cooled to the same baseplate.

The nominal spent beam refocuser consisted of two full-strength permanent magnets (in a continuation of the periodic permanent magnet stack) past the RF output of the TWT, and required only the addition of a single magnet to the output end of the production model TWT.

MDC Assembly Design and Fabrication

Basic Electrode Material

The collector electrodes were made of Poco Graphite Inc., grade DFP-2 isotropic graphite, which is an ultrafine grain, high purity, readily machinable material having other distinctive advantages as well (Data sheet for DFP-2, Semiconductor Metallurgical Grades, Poco Graphite, Inc., Decatur, Texas, January 1, 1978). The material has an open and interconnecting porosity, which expedites outgassing during vacuum bakeout. Its coefficient of thermal expansion

is such that direct brazing to alumina (and beryllia) is possible. The impurity level is less than 5-ppm ash content. It has relatively good (low) secondary electron emission characteristics from machined surfaces, and can be readily textured to produce a surface with extremely low secondary electron emission characteristics (ref. 5).

Design Concepts and Fabrication Techniques

The MDC used the fabrication techniques and the modular design concept described in detail in reference 3. Figure 2 illustrates how each module, representing a single electrode, was built as a brazed composite with a centrally located graphite electrode, which was electrically isolated with a ceramic ring from the thin metal outer sheath. Final machining of the graphite electrodes was done after completion of the braze operations. The edges of the outer ring of each of the electrode modules and the electrical feedthrough element were prepared with matching butt-lap joints to provide self-fixturing weld connections and concentric alignment of the electrodes. The individual components which made up the entire MDC assembly, except for internal wiring and ion pump, are shown in figure 3. The electrode modules, together with the HV feedthrough assembly and TWT output flange, were stacked to create the multiple-tiered arrangement as shown in figure 4, and joined by electron beam welds to make the final vacuum-tight closures. The finished MDC assembly, joined to the TWT body by welds and mounted onto the baseplate, is shown in figure 5.

Performance Evaluation

The TWT body was added to the MDC without any previously documented TWT performance (P_{RF} and P_b as functions of frequency, and P_b as a function of P_{RF} at a given frequency) with an undepressed collector. Consequently, as discussed in reference 6, the computation of collector efficiencies required some assumptions as to the true intercepted beam power and circuit losses (the sum of which is P_b) at various TWT operating conditions. In this report it was assumed that the experimental TWT (MTH 5065, S/N 001) exhibited the same beam interception and circuit loss characteristics as those reported in reference 7 for model MTZ-7000 S/N 103, a TWT of virtually identical design. Since the computed collector efficiencies were not based on directly measured values of P_b for the same TWT, they were labeled as "estimated collector efficiencies."

Filtered input drive at the fundamental frequency was used throughout these tests. Saturation was determined by using an uncalibrated power meter which, by means of a low-pass filter, measured RF power only at the fundamental frequency. However, only the total RF power, P_{RF} , (including any harmonic power) that was dissipated in the water-cooled matched load was measured, and all TWT overall and electronic efficiencies reported here are based on this P_{RF} .

TABLE I.—GENERAL CHARACTERISTICS OF T MEC
TWT MODEL MTH-5065

Frequency, f , GHz	4.8 to 9.6
Cathode voltage, V_0 , kV	9.75
Cathode current, I_0 , A	0.38
Perveance, $A/V^{3/2}$	$.39 \times 10^{-6}$
RF efficiency, η_{RF} , percent	16 (maximum)
Focusing	Periodic permanent magnet (PPM)
Duty cycle, percent	100

Although the MDC geometry had been optimized (by the computer-aided design technique described in ref. 2) for operation as a four-stage collector, the MDC was operated in the three-stage configuration as well. The number of collector stages is defined as the number of distinct voltages (other than ground) required to operate the MDC. In the three-stage configuration, electrodes 1 and 2 (see fig. 1) were operated at identical potentials.

Performance Optimization

A newly developed performance optimization system was used to optimize the TWT overall efficiency. This device, which includes a HV unit inserted between the MDC and its power supply (fig. 6), is compatible with all types of power supplies since the HV unit is a series element external to the power supply. The HV unit measures the collector voltages (V_{en} 's) and the currents (I_{en} 's) under both pulsed and CW operating conditions. The current signals are coupled out to a grounded analog computer by means of four optical fiber links for a four-electrode collector by using a novel optical signal isolation technique (ref. 8). In the pulsed mode, four additional fiber links are required to trigger the sampling point at the desired portion of the waveform. The collector voltages are measured by using resistive dividers grounded at one end. The "instantaneous" power recovered by the collector, P_{rec} , is displayed on a digital voltmeter.

The optimization system was first used in the final focusing (shunting) of the periodic permanent magnet stack of the TWT. Parameters P_{rec} , I_G , and P_{RF} were monitored during this operation. It had been previously observed that (at constant P_{RF}) the addition of shunts which lowered I_G did not necessarily increase P_{rec} ; however, locations for shunts could be found where both I_G and P_{rec} improved. In the present case the final focusing was used to boost the RF output power by 2 to 3 percent while maintaining the same P_{rec} and the same (already low) I_G . This resulted in the improvement of the overall efficiency by a similar amount. After final focusing of the tube, TWT-MDC performance optimization was limited to optimization of the MDC operating voltages for broadband operation at saturation. Optimization of the refocusing system by trimming the strength of the two permanent magnets was not attempted, since very good results were obtained at the nominal values (ref. 4).

Results of Bakeout and Processing

The TWT-MDC was baked for 65 hr at 500 °C. In terms of outgassing performance the TWT-MDC was indistinguishable from production TWT's with copper electrode collectors. It took 350 hr of pulsed operation to bring the TWT-MDC up to CW operation. However, most of the gas seemed to originate in the TWT body, possibly due to the fact that the TWT body had been assembled and stored for about one year before the MDC became available. Moreover,

a very conservative approach was taken with this TWT-MDC as to the level of ion pump current which was not to be exceeded. Consequently, no new information of any significance concerning the processing requirements of the isotropic graphite MDC was derived from this test.

Multistage Depressed Collector Test Results

TWT-MDC Performance at Saturation

The saturated RF output power and the TWT body power, P_b , used to compute estimated collector efficiencies as functions of frequency are shown in figure 7. The RF and overall efficiencies as functions of frequency for both the four- and three-stage collector hook-ups are shown in figure 8. The corresponding collector efficiencies as functions of frequency are shown in figure 9. The collector efficiencies are relatively insensitive to the operating frequency. The results are summarized in table II. The average overall and collector efficiencies (across the operating band at saturation) were 43.8 and 82.6 percent, respectively, with the four-stage collector and 40.6 and 79.7 percent with the three-stage collector. The three-stage results are not necessarily optimum since the collector geometry was not independently optimized for three-stage operation. The four-stage collector results are comparable to those obtained with the same basic TWT model in combination with spent beam expansion and collimation, and an MDC of similar size with carbon-black coated electrodes (ref. 1). The normalized collector operating voltages with respect to V_0 are shown in table III.

TABLE II.—SUMMARY OF TWT AND MDC PERFORMANCE AT SATURATION ACROSS OPERATING BAND OF 4.8 to 9.6 GHz

Number of MDC stages	Average RF efficiency, percent	Average overall efficiency, percent	Average collector efficiency, percent	Maximum dc input power, W
4	13.9	43.8	82.6	1240
3	13.9	40.6	79.7	1340

TABLE III.—MDC OPERATING VOLTAGES NORMALIZED WITH RESPECT TO CATHODE VOLTAGE (OPTIMIZED FOR BROADBAND OPERATION AT SATURATION)

MDC electrode number	Four-stage normalized voltage	Three-stage normalized voltage
1	0.533	0.533
2	.656	.533
3	.852	.836
4	1.00	1.00

TWT-MDC Current and dc Input Power Distributions at Saturation

The TWT-MDC currents and dc input powers as functions of frequency for the four-stage collector are shown in figures 10 and 11, respectively. The corresponding distributions for the three-stage collector are shown in figures 12 and 13, respectively. The maximum values for each current-collecting element, together with the operating voltage, define the power conditioning requirements for saturated operation of the TWT.

TWT-MDC Performance Over TWT Dynamic Range

The TWT overall efficiency and collector efficiency as functions of RF output power at the operating frequency (8.0 GHz) corresponding to the highest RF efficiency at saturation are shown in figures 14 and 15, respectively. The MDC operating conditions (voltages) used were identical to those used for saturated operation. For both collectors, MDC efficiency rose steadily (but very slowly) for TWT operation increasingly below saturation, and a reasonable overall efficiency (>20 percent) could be maintained for TWT operation as much as 6 dB below saturation. The collector efficiencies, for operation of the TWT in the low end of the linear range, were severely limited by the potential (optimized for saturation) of the second most depressed electrode. These values were 0.85 and 0.84 V_0 for the four- and three-stage collectors, respectively. No attempt was made to optimize these collectors for only linear operation of the TWT.

TWT-MDC Current and dc Input Power Distributions Over TWT Dynamic Range

The TWT and four-stage collector currents and dc input powers as functions of RF output power at 8.0 GHz are shown in figures 16 and 17, respectively. The corresponding distributions for the three-stage collector are shown in figures 18 and 19, respectively.

For both collectors the maximum value of current collected by and the dc input power supplied to one of the electrodes (electrode 3) occurred at the low end of the linear range.

Concluding Remarks

The performance of a computer designed, small-sized, isotropic graphite electrode MDC was evaluated in conjunction with a 500-W octave bandwidth TWT. A full-strength permanent magnet spent-beam refocuser (consisting of a continuation of the periodic permanent magnet stack for 1 1/4 periods past the RF output of the TWT) was used. This permitted complete (axial) beam debunching (and modeling),

but no radial beam expansion before injection into the collector. A novel performance optimization system was used to optimize the TWT-MDC performance for saturated, broadband CW operation. The average overall and collector efficiencies of 43.8 and 82.6 percent, respectively, for saturated operation of the TWT over its octave bandwidth slightly exceeded those obtained with the same basic model TWT in an earlier laboratory demonstration involving a variable beam expander and collimator and carbon-black coated MDC electrodes. The TWT-refocuser-MDC assembly fit within the envelope of the production model TWT and was conductively cooled to the same baseplate.

The isotropic graphite shows considerable promise as an MDC electrode material because of its high purity, low cost, potential for very compact overall MDC size, and relatively low secondary-electron-emission yield characteristics in the as-machined state. However, little new information on its outgassing characteristics or long-term stability was derived from the present test, and considerably more test experience is required before definitive conclusions on its suitability for space or airborne TWT's can be made.

Lewis Research Center

National Aeronautics and Space Administration

Cleveland, Ohio, November 6, 1987

References

1. Ramins, P.; and Fox, T.A.: Performance of Computer-Designed Small Sized Four-Stage Depressed Collector for Operation of Dual-Mode Traveling Wave Tube. NASA TP-1832, 1981.
2. Ramins, P., et al.: Verification of an Improved Computational Design Procedure for TWT-Dynamic Refocuser MDC Systems with Secondary Electron Emission Losses. IEEE Trans. Electron Dev., vol. 33, no. 1, Jan. 1981, pp. 85-90.
3. Ebihara, B.T.; and Ramins, P.: Design, Fabrication and Performance of Small, Graphite Electrode, Multistage Depressed Collectors With 200-W, CW, 8- to 18-GHz Traveling-Wave Tubes. NASA TP-2693, 1987.
4. Ramins, P.; Force, D.A.; and Kosmahl, H.G.: Analytical and Experimental Performance of a Dual-Mode Traveling-Wave Tube and Multistage Depressed Collector. NASA TP-2752, 1987.
5. Curren, A.N.; and Jensen, K.A.: Secondary Electron Emission Characteristics of Ion-Textured Copper and High-Purity Isotropic Graphite Surfaces. NASA TP-2342, 1984.
6. Kosmahl, H.G.: Comments on Measuring the Overall and the Depressed Collector Efficiency in TWT's and Klystron Amplifiers. IEEE Trans. Electron Dev., vol. 26, no. 2, Feb. 1979, p. 156.
7. Ramins, P.; and Fox, T.A.: Multistage Depressed Collector with Efficiency of 90 to 94 Percent for Operation of a Dual-Mode Traveling Wave Tube in the Linear Region. NASA TP-1670, 1980.
8. Lesny, G.G.: TWT Test Set with Optical High Voltage Signal Isolation. Patent Disclosure NASA Case No. LEW-14, 529-1, 1987. (U.S. Patent Applied for.)

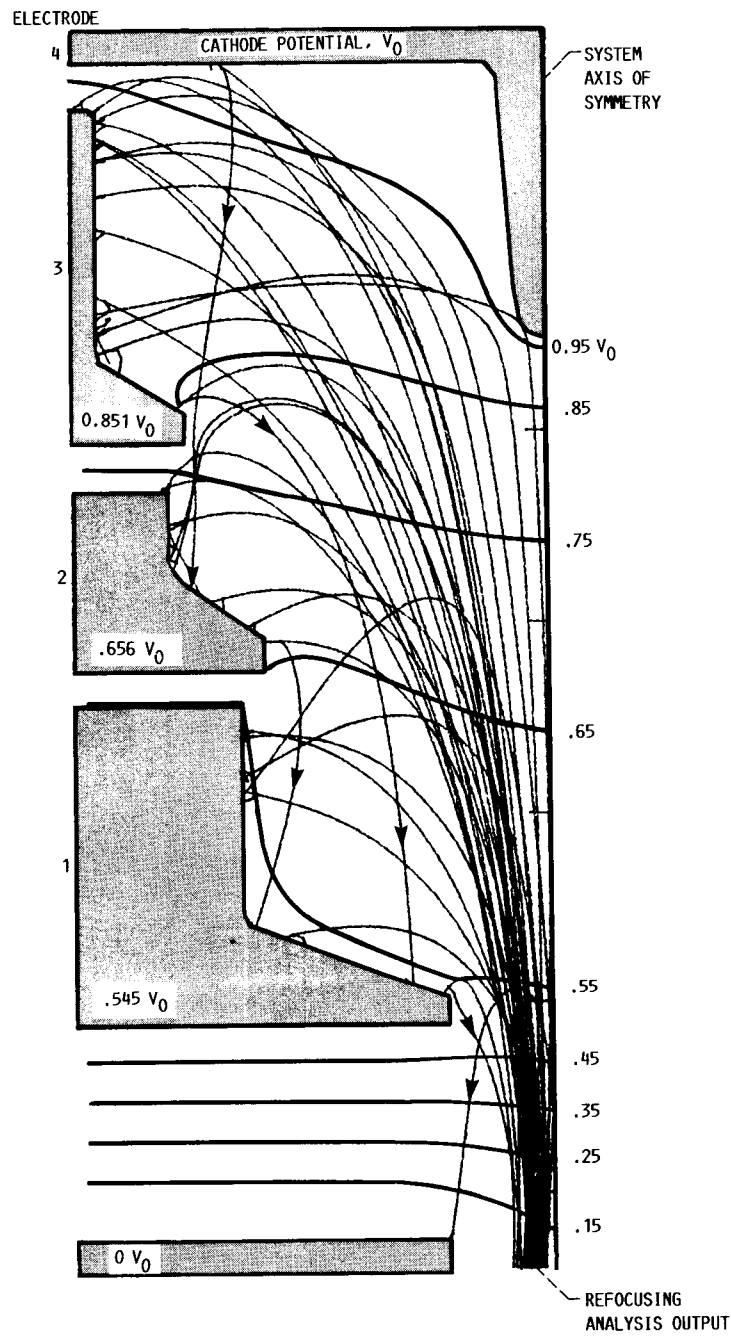


Figure 1.—Trajectories of primary and secondary electron emission charges in four-stage, 2.4-centimeter-diameter collector operating at experimentally optimized voltages for TWT operating at saturation at 8.4 GHz in low mode.

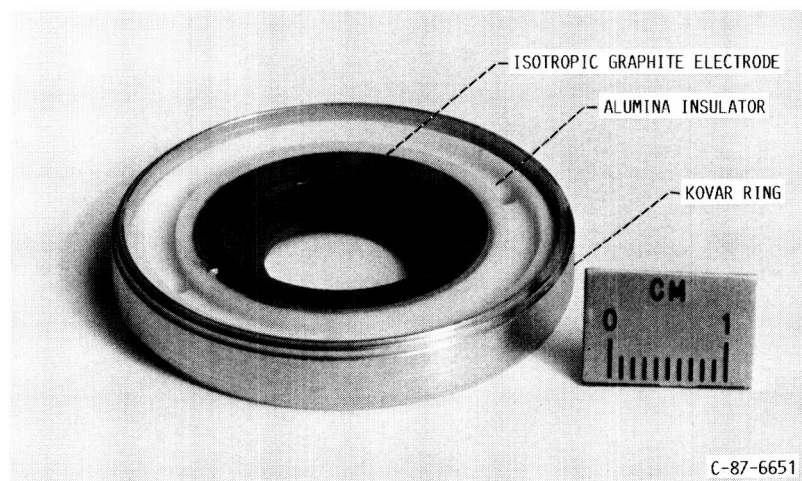


Figure 2.—Typical all-brazed electrode module showing isotropic graphite electrode, alumina insulator, and Kovar-metal outer ring.

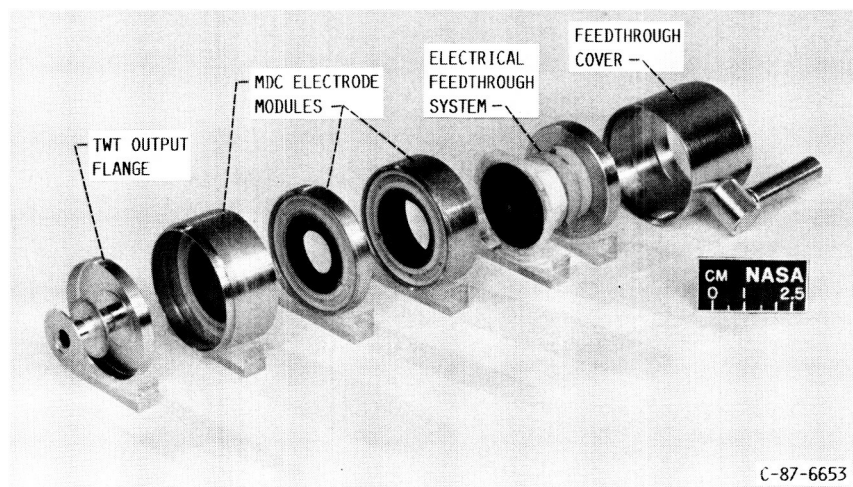


Figure 3.—Exploded view of four-stage, isotropic graphite electrode depressed collector ready for final assembly by welding.

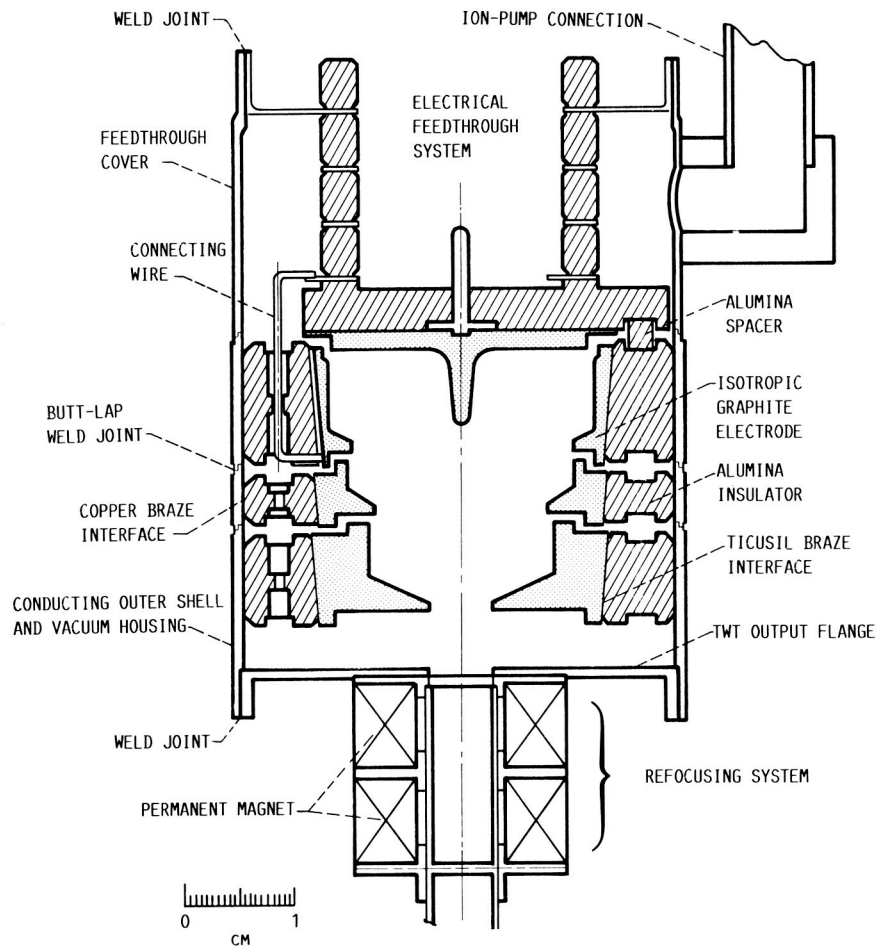


Figure 4.—Cross section of four-stage, brazed, isotropic graphite electrode depressed collector and permanent magnet refocusing system.

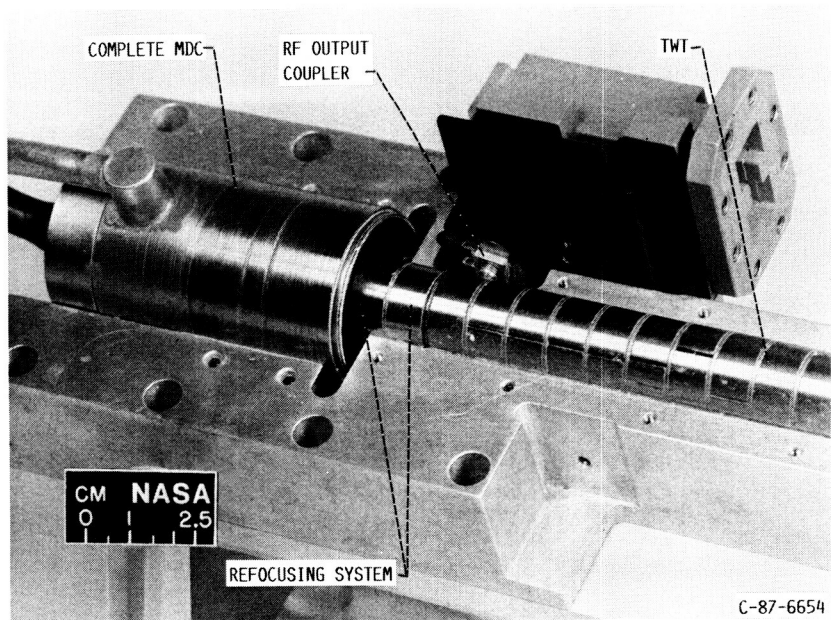


Figure 5.—Fully assembled TWT and collector cradled within a baseplate.

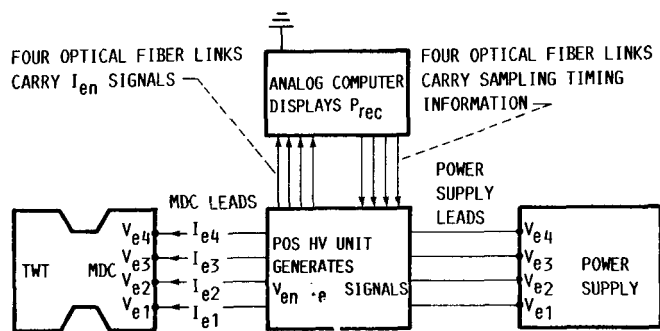


Figure 6.—Functional block diagram of the performance optimization system (POS) used to maximize the TWT overall and collector efficiencies under pulsed or CW operating conditions. It is compatible with all types of power supplies.

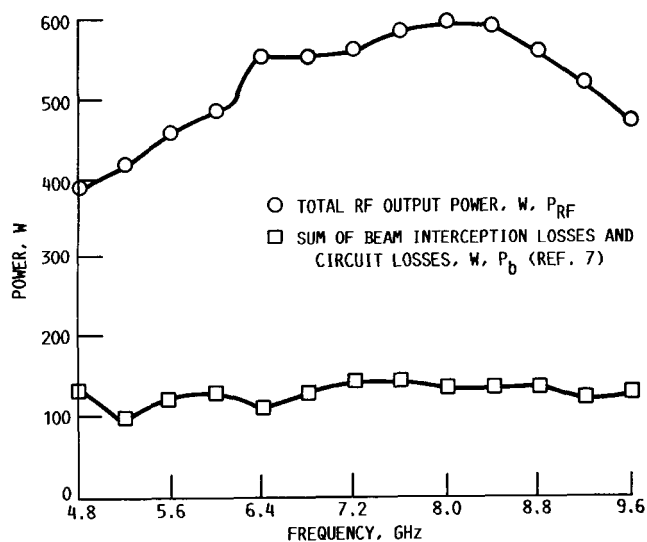


Figure 7.—RF and TWT body powers as functions of frequency at saturation.

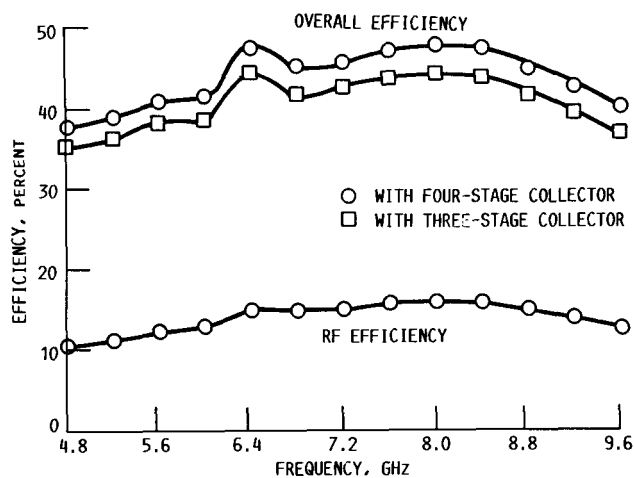


Figure 8.—Overall and RF efficiencies as functions of frequency at saturation.

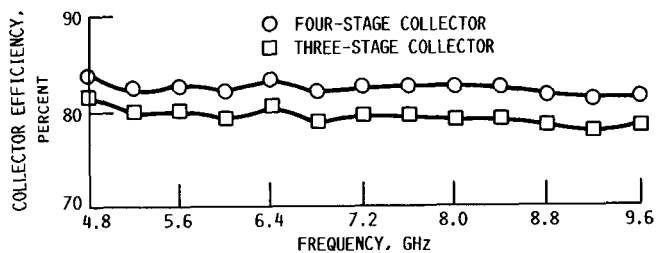


Figure 9.—Estimated collector efficiency as function of frequency at saturation.

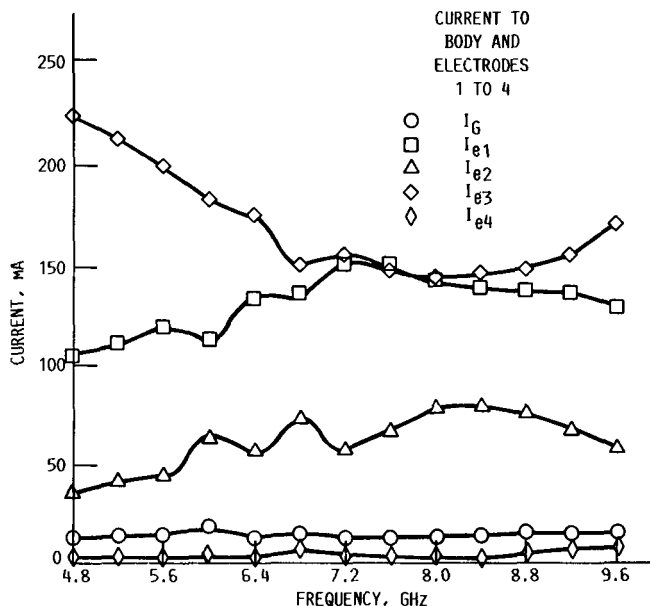


Figure 10.—Four-stage collector electrode current distribution as function of frequency at saturation.

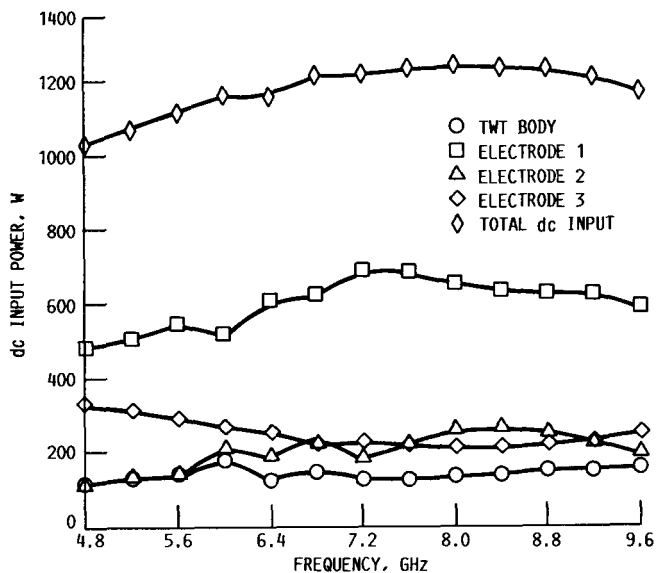


Figure 11.—Direct current input power per electrode in four-stage collector as function of frequency at saturation.

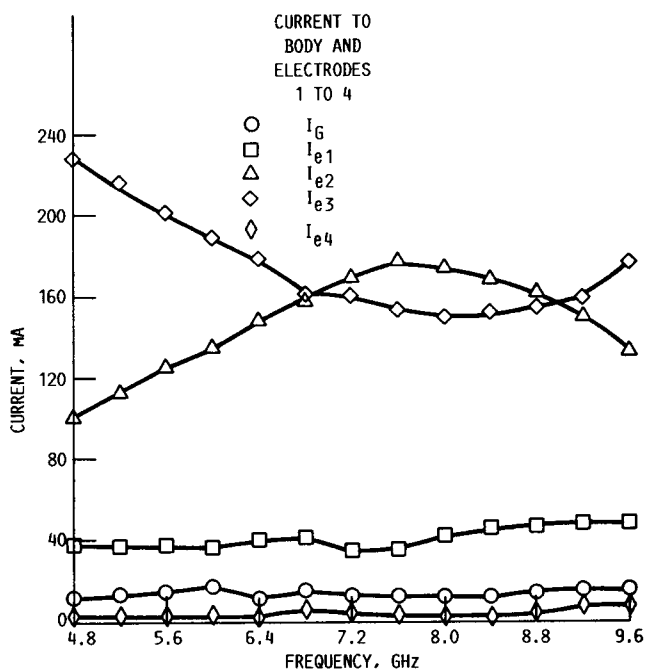


Figure 12.—Three-stage collector electrode current distribution as function of frequency at saturation.

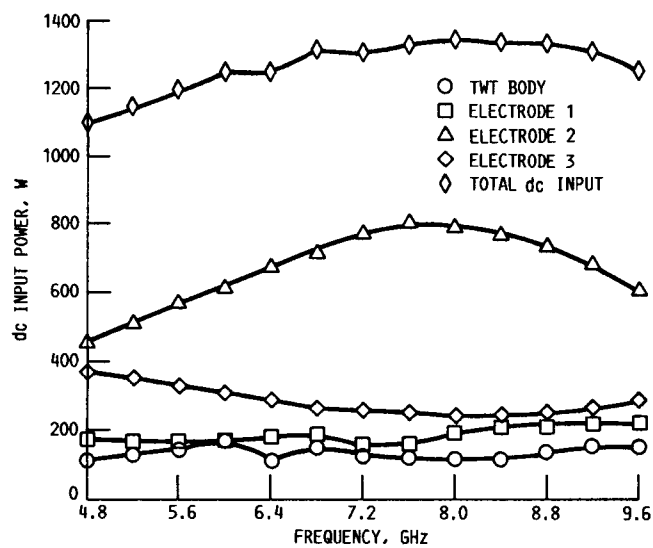


Figure 13.—Direct current input power per electrode in three-stage collector as function of frequency at saturation.

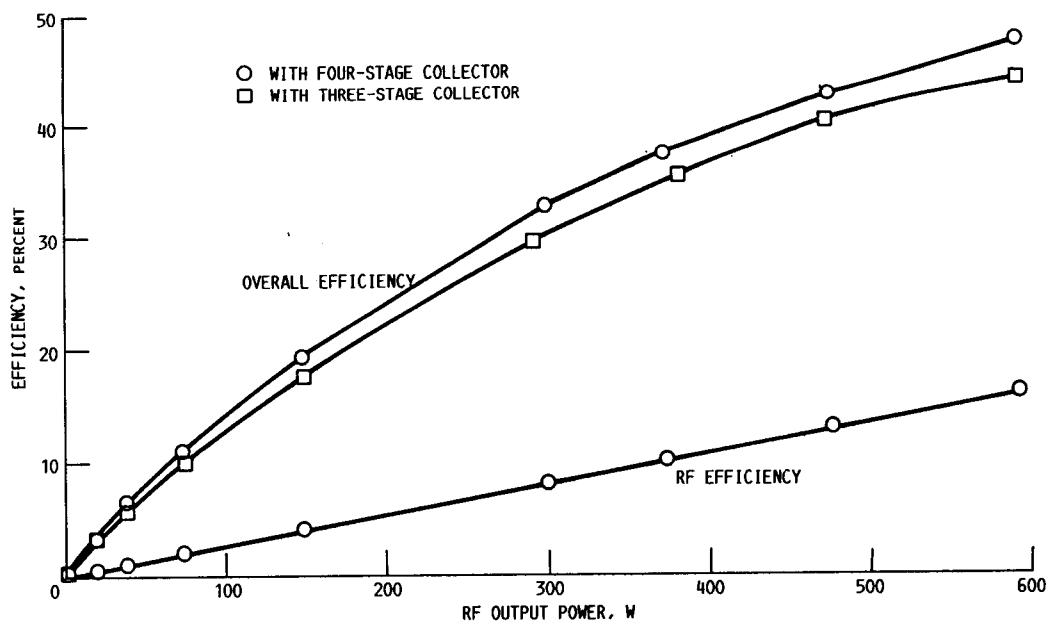


Figure 14.—Overall and RF efficiencies as functions of RF output power at 8.0 GHz.

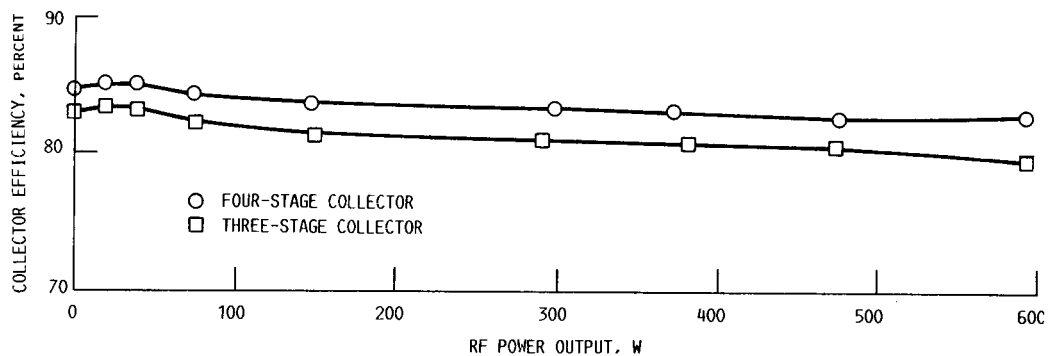


Figure 15.—Estimated collector efficiency as function of RF output power at 8.0 GHz.

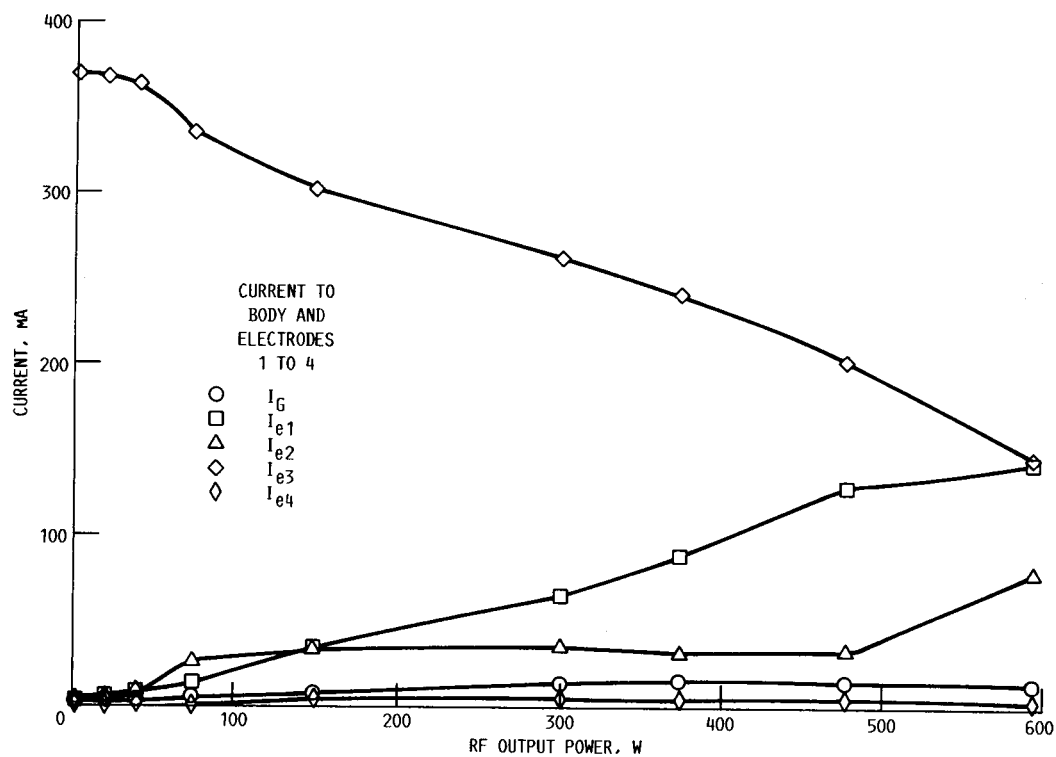


Figure 16.—Four-stage collector electrode current distribution as function of RF output power at 8.0 GHz.

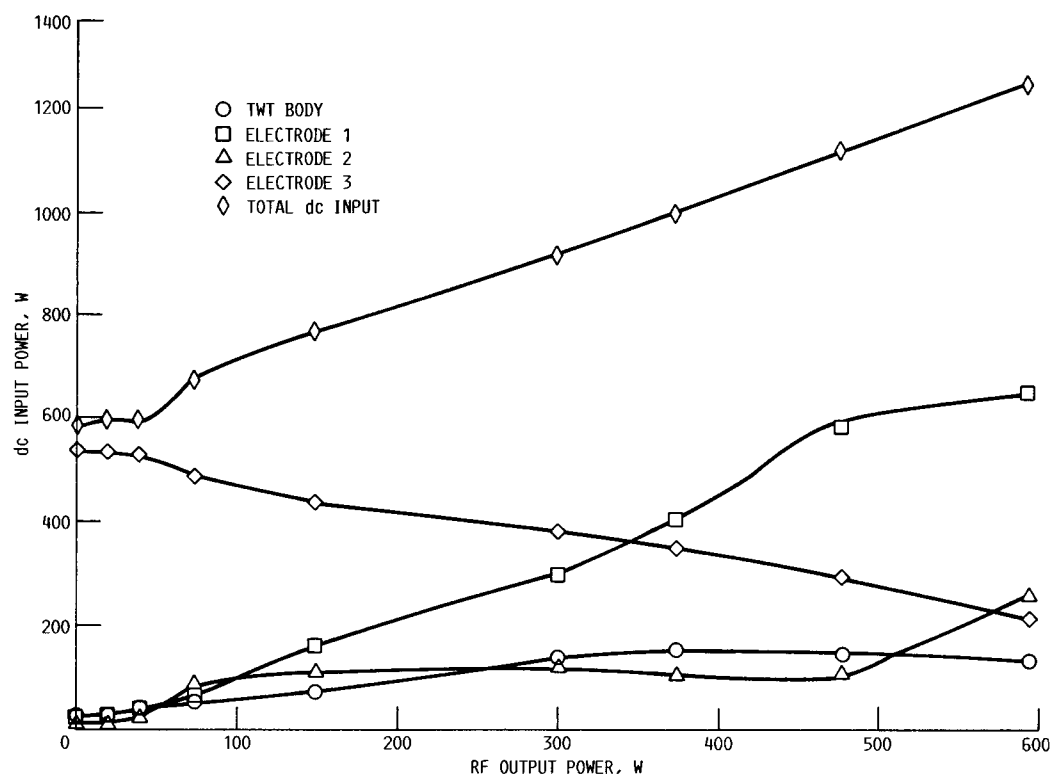


Figure 17.—Direct current input power per electrode in four-stage collector as function of RF output power at 8.0 GHz.

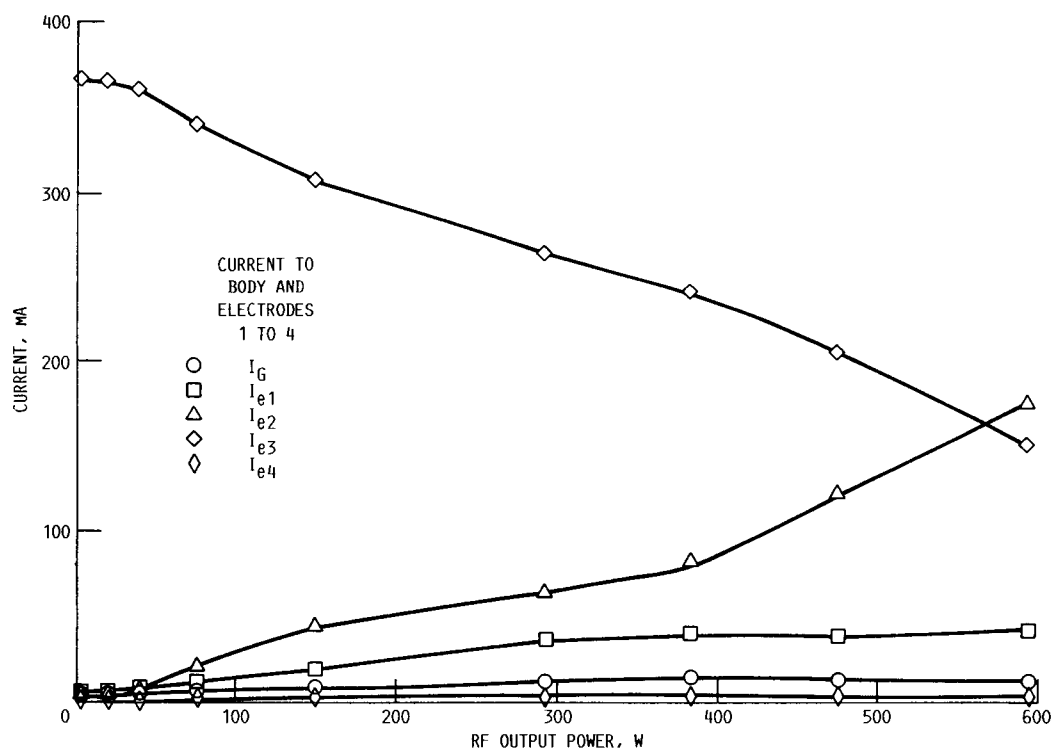


Figure 18.—Three-stage collector electrode current distribution as function of RF output power at 8.0 GHz.

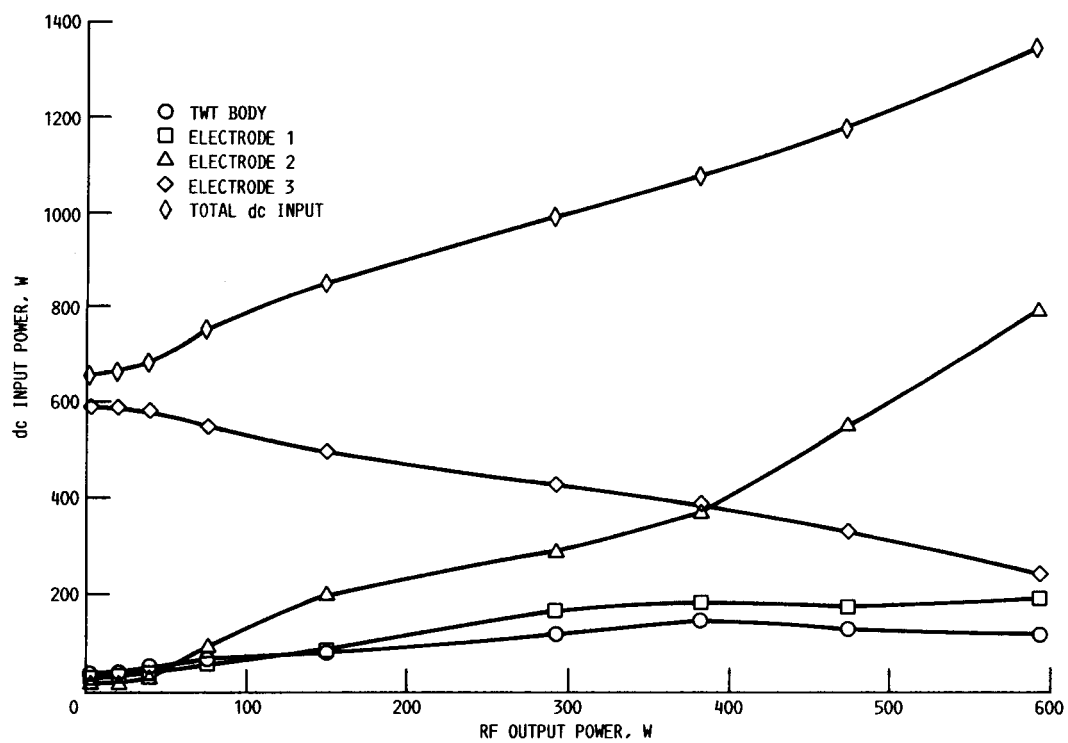


Figure 19.—Direct current input power per electrode in three-stage collector as function of RF output power at 8.0 GHz.

Report Documentation Page

1. Report No. NASA TP-2788		2. Government Accession No.		3. Recipient's Catalog No.	
4. Title and Subtitle Performance of a Small, Graphite Electrode, Multistage Depressed Collector With a 500-W, Continuous Wave, 4.8- to 9.6-GHz Traveling Wave Tube				5. Report Date February 1988	
				6. Performing Organization Code	
7. Author(s) Peter Ramins, Gary G. Lesny, Ben T. Ebihara, and Shelly Peet				8. Performing Organization Report No. E-3800	
				10. Work Unit No. 506-44-21	
9. Performing Organization Name and Address National Aeronautics and Space Administration Lewis Research Center Cleveland, Ohio 44135-3191				11. Contract or Grant No.	
				13. Type of Report and Period Covered Technical Paper	
12. Sponsoring Agency Name and Address National Aeronautics and Space Administration Washington, D.C. 20546-0001				14. Sponsoring Agency Code	
15. Supplementary Notes P. Ramins, G.G. Lesny, B.T. Ebihara, Lewis Research Center; Shelly Peet, student intern with the Case-NASA Cooperative Aerospace R&D Fellowship Program.					
16. Abstract A small, isotropic graphite multistage depressed collector (MDC) and a short permanent magnet refocuser were designed, fabricated, and evaluated in conjunction with a 500-W, continuous-wave (CW), 4.8- to 9.6-GHz traveling wave tube (TWT). A novel performance optimization system and technique were used to optimize the TWT-MDC performance for saturated broad-band operation. The MDC performance was evaluated in both four- and three-stage configurations. Average TWT overall and four-stage collector efficiencies of 43.8 and 82.6 percent, respectively, were obtained for saturated octave-bandwidth operation. The isotropic graphite electrode material performed well, and shows considerable promise. However, considerably more test experience is required before definitive conclusions on its suitability for space or airborne TWT's can be made.					
17. Key Words (Suggested by Author(s)) Traveling-wave tube Multistage depressed collector Graphite electrodes			18. Distribution Statement Unclassified - Unlimited Subject Category 33		
19. Security Classif. (of this report) Unclassified		20. Security Classif. (of this page) Unclassified		21. No of pages 14	
				22. Price* A02	